

Article

Micromagnetic Analysis of Thermally Induced Influences on Surface Integrity Using the Burning Limit Approach

Jonas Heinzl ^{1,2,*}, Daniel Sackmann ² and Bernhard Karpuschewski ^{1,2}

¹ MAPEX Center for Materials and Processes, University of Bremen, Bibliothekstraße 1, 28359 Bremen, Germany; karpuschewski@iwt-bremen.de

² Leibniz Institute for Materials Engineering IWT Bremen, Division Manufacturing Technologies, Badgasteiner Straße 3, 28359 Bremen, Germany; sackmann@iwt-bremen.de

* Correspondence: jheinzl@iwt-bremen.de

Received: 11 October 2019; Accepted: 7 November 2019; Published: 12 November 2019



Abstract: Particularly for highly stressed components, it is important to have precise knowledge of the surface and subsurface properties and, thus, of the functional properties after final grinding at the end of a complex process chain in order to avoid rejected parts. Therefore, non-destructive testing methods have been the subject of research for several years. The Barkhausen noise analysis, as a micromagnetic measuring method, has the potential to characterize the subsurface area up to an analyzing depth δ non-destructively with micromagnetic parameters. In addition to micromagnetic multiparameter approaches, which allow post-process mode clear statements about the subsurface area state, the present research work deals with the concept of a connection of a single Barkhausen noise parameter with grinding process parameters. In combination with the analytical approach of Malkin for the thermal surface and subsurface area influence, which is based on the process parameters of grinding processes, a distinction between good and rejected ground parts can be achieved. The results show that, by post-process measurements of the Barkhausen noise on case-hardened workpieces made of steel 18CrNiMo7-6 (No. 1.6587, AISI 4820) and machined by a cylindrical grinding process, incipient changes in the residual stress state up to industrial-relevant limits, which distinguish between good and rejected parts, is possible. In the future, a combination of the Malkin grinding burning limit and sufficient condition monitoring based on in-process measurements of Barkhausen noise will be investigated. The application limits of the analytical approach of Malkin as well as the measurement of the Barkhausen noise in-process have to be determined.

Keywords: grinding; burning limit; Barkhausen noise; analytical approach; residual stress state

1. Introduction and State of the Art

Highly stressed components, such as powertrain components, are usually heat-treated in order to adjust the strength of the microstructure for the corresponding load [1]. Case-hardened steels are widely used, especially in drive technology. After heat treatment, workpieces are usually processed by grinding at the end of the process chain to produce high dimensional and shape accuracy and high-quality surfaces [2–5]. In addition to geometric parameters, thermomechanical loads during grinding also determine the surface and subsurface properties and, thus, the functional properties of the finished workpiece [6,7]. For selected testing of the surface and subsurface properties after grinding, destructive measuring methods (e.g., X-ray residual stress measurements and metallographic inspection) are well-established and widely used [5]. Non-destructive methods have been the subject of research for several years. The Barkhausen noise (BN) analysis, as a micromagnetic measuring

method, has the potential to characterize the surface and subsurface layers non-destructively with micromagnetic parameters [2,4,5].

Micromagnetic Barkhausen Noise Analysis

Figure 1 shows a typical measurement setup for BN measurements as a sketch. With an excitation coil (outer upper coil), an alternating magnetic field H is generated in the material, and the resulting magnetic flux density B is detected via a receiving coil or a Hall sensor. A remagnetization of individual micromagnetic domains (called Weiss domains) are affected by discontinuous, stepwise displacements of the Bloch walls when the respective remagnetization field strength is exceeded [8]. Since the orientation and the remagnetization energy of the Weiss domains are stochastically distributed on a macroscopic scale, the continuous field strength progression in the material is superimposed by a signal resulting from the displacement of the Bloch walls, the so-called BN [8].

The BN is attenuated exponentially as a function of the depth reached in the material. This attenuation is mainly caused by the eddy current attenuation of electromagnetic fields [9–11] that are generated around the moving Bloch walls. The depth δ of the BN measurement can be estimated as follows (Equation (1)) [10]:

$$\delta = \frac{1}{\sqrt{\pi\mu_0\mu_r\sigma f_a}} \tag{1}$$

Essentially, the depth δ therefore depends on the analysis frequency f_a , the conductivity σ , and the permeabilities μ_r und μ_0 .

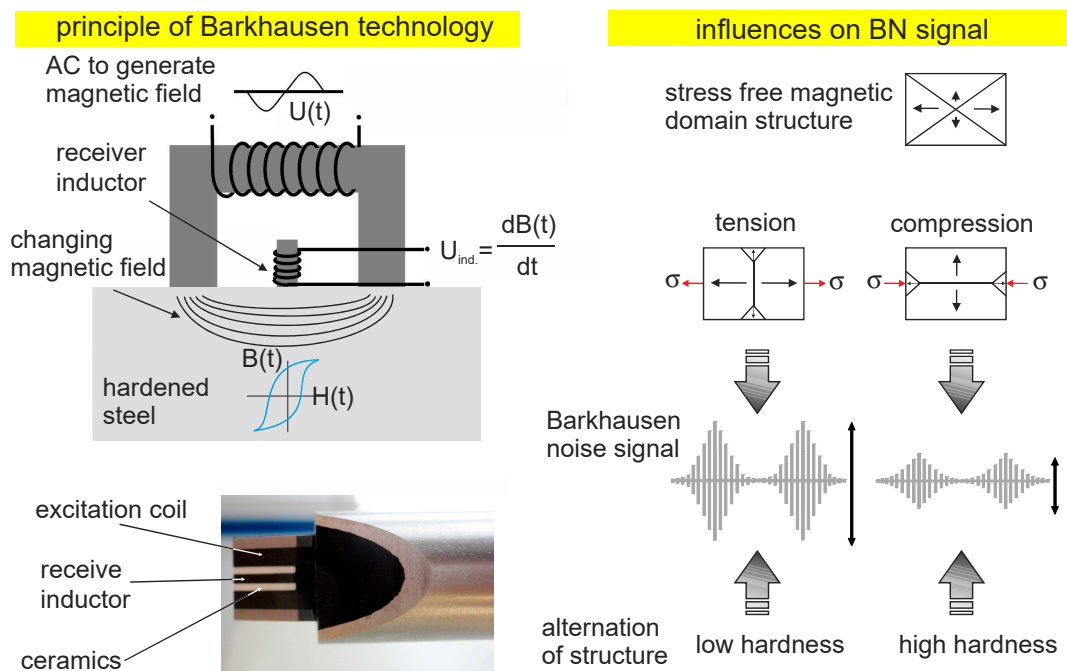


Figure 1. The measuring principle for measuring the Barkhausen noise of ferromagnetic materials and typical signals for different materials according to References [4,5].

In the past, individual micromagnetic parameters (in particular the BN amplitude) for the assessment of ground workpieces, have often been tested for correlation with the residual stress state, hardness, dislocation density, and chemical homogeneity of the microstructure [2,5,12,13].

If the surface and subsurface layers of a workpiece exhibit reduced hardness or tensile residual stresses due to the thermal damage, the level of the BN signal increases [4,14]. More than 20 years ago the suitability of the method for grinding burn testing was shown [4,15]. Using 3MA test equipment from the Fraunhofer Institute for Nondestructive Testing (IzFP), Saarbrücken, Germany, quantitative

investigations of hardness and residual stresses were carried out in References [4,16]. In Reference [17], the grindability of case-hardened steels was investigated and the BN was used to detect damage. Two different materials (20MnCr5: No. 1.7147; AISI 4820; and 18CrNiMo7-6) and two different case hardening depths (CHDs) were used. Further research is described in Reference [7], where two micromagnetic methods were used to perform a grinding burn test and quantitative hardness and residual stress measurements after grinding. The investigations show that a correct interpretation of the BN signal as well as other micromagnetic parameters requires calibration on the basis of good and bad parts, even for a qualitative evaluation. The surface and subsurface condition of these parts must be exactly defined with alternative test methods and assigned to the respective BN level [18]. The reason for this is the fact that the surface and subsurface state is defined by different surface and subsurface properties (e.g., residual stress state, hardness, microstructure), so that changes in several properties simultaneously cause overlapping micromagnetic effects. Thus, the measurement result of the BN amplitude cannot be clearly assigned to the change of a certain surface and subsurface property. In order to obtain meaningful results based on the measurement of micromagnetic parameters, micromagnetic multiparameter approaches came into focus.

In 1995, for example, Karpuschewski [4] developed a classification scheme for ground, case-hardened components with regard to possible surface and subsurface damage by combining various micromagnetic parameters of the 3MA equipment technology. This allowed for fast post-process grinding burn detection. A non-destructive, objective, quick, and economical detection of grinding errors was achieved with this device technology [2,19]. Both, the occurrence of tempering zones and the formation of re-hardened zones can be determined [2]. In 1996, Suominen and Wojtas [10] presented a comparative study of BN and X-ray diffraction measurements on ground ferritic steel samples based on the Rollscan device technology by Stresstech. In addition to the root mean square value of the BN amplitude, other micromagnetic parameters were evaluated [10]. Thus, an increase of the parameter called “peak position” was accompanied by a higher hardness. Thiemann [20] presented a two-parameter approach based on Stresstech device technology in 2019 which enables a clear non-destructive characterization of the machined surface, even if re-hardened zones or retained austenite transformations occur which lead to overlapping micromagnetic effects. For workpieces of case-hardened steel 18CrNiMo7-6, a large number of gradations of thermo-mechanically damaged surface and subsurface changes were produced by an external cylindrical grinding process. These gradations were generated by taper grinding over the circumference of the workpiece [1,20]. In these tests, the depth of cut a_e continuously increased during a total of one workpiece revolution. In addition to the root mean square value, Thiemann et al. [1] used the peak position parameter to determine the differences. This describes the position of the maximum BN and, thus, the coercivity H_{cM} . Further information about the micromagnetic parameters of the Rollscan device are provided in Reference [21].

Besides the investigation of multiparameter approaches, Karpuschewski et al. [22,23] also tried to detect BN in-process. Due to the lack of protective layers, the sensor showed serious signs of wear and impairment in the workpiece surface. This is where the research approach described above becomes useful. As a result of the development of sensor technology and the application of a wear protection layer on the sensors, this approach is now being revisited. In combination with the analytical approach of Malkin [24,25] for the thermal surface and subsurface area of influence, which is based on the process parameters of the grinding process, a distinction between good and rejected ground parts can be achieved.

2. Motivation and Research Approach

Barkhausen noise, as a non-destructive testing method, is of significant importance, especially in grinding technology when reliable and reproducible statements are needed regarding the surface and subsurface state of ground workpieces. However, due to the opposing effects caused by the different micromagnetic properties of different surface and subsurface properties, ambiguities in quantitatively determined micromagnetic characteristic values often prevent unambiguous statements. Therefore,

the aim of this work was a combined evaluation of several measured micromagnetic parameters. An alternative to this evaluation method is in-process measuring of the BN level during grinding. By measuring the BN amplitude continuously during processing, the corresponding micromagnetic parameter can be unambiguously interpreted even without measuring further parameters. In the following, the stress sensitivity of the BN on case-hardened and machined 18CrNiMo7-6, in combination with the analytical model for the thermal surface and subsurface area influence of Malkin, was considered. The aim was to make a clear statement about the surface and subsurface state of the ground workpiece to distinguish between a good and a rejected part.

Analytical Model for Thermal Surface and Subsurface Area Influence According to Malkin
Malkin's [24,25] approach is based on the analysis of the specific grinding energy e_c ; this is calculated from the quotient of the grinding power P_c and the material removal rate Q_w , where v_c is the cutting speed and F_t the tangential force.

$$e_c = \frac{P_c}{Q_w} = \frac{F_t \cdot v_c}{Q_w} \quad (2)$$

The grinding energy is composed of the energy components for chip formation, plowing, and sliding [25,26].

$$e_c = e_{chip} + e_{plough} + e_{fric} \quad (3)$$

If the proportion of the grinding energy is considered which flows into the workpiece surface and is converted into heat, it can be assumed that the maximum temperatures in the shear plane reach the melting temperature range of the processed material. However, these extreme temperatures only occur locally, whereas thermally induced surface and subsurface influences occur on a plane. This plane is considerably larger than the chip formation plane. Thus, these maximum temperatures can be neglected when the contact zone temperature is estimated. In order to calculate this temperature, Jaeger [27] assumes that the contact zone moves over the workpiece surface as a heat source during grinding [26,27]. According to Jaeger [27], the maximum dimensionless surface temperature is calculated as:

$$\bar{\theta}_m = \frac{\pi \cdot k \cdot V}{2 \cdot a \cdot q} \cdot \theta_m = 3.543 \cdot L^{0.5} \text{ with } L = \frac{Vl}{2a} \quad (4)$$

Taking into account the geometrical conditions of cylindrical grinding, the energy distribution and the thermal properties of steels, the critical specific grinding energy e_c^* can be calculated for a given critical temperature θ_m^* at which grinding burn occurs [25,26].

$$e_c^* = e_w + B \cdot d_{eq}^{0.25} \cdot a_e^{-0.75} \cdot v_w^{-0.5} \quad (5)$$

Malkin [25] investigated various flat and cylindrical grinding processes and determined the specific grinding energy for the point where grinding burn occurs. If these energies are plotted over the product $d_{eq}^{0.25} a_e^{-0.75} v_w^{-0.5}$ from Equation (5), factor B can be determined by linear regression to 7.2 J/(mm²·s^{0.5}) (or 8.8 J/(mm²·s^{0.5}) with graphical determination) from the diagram shown in Reference [25]. Taking into account the thermal properties of steel, it can be determined that the critical temperature leading to the occurrence of grinding burn is approximately $\theta_m^* = 650$ °C [25,26].

Figure 2 shows the linear grinding burn limit for the two different factors B according to Malkin [25]. The area between the two linear lines for the burning limits is colored grey and is regarded as a transition area in the following. In addition, grinding burn limits from taper grinding on disks made of case-hardened steel 18CrNiMo7-6 from Reference [6] are plotted. This special external cylindrical grinding process, in which the depth of cut increases continuously during one workpiece revolution, leads to a critical temperature being reached after the grinding burn limit, as a result of the critical depth of cut being exceeded. In Reference [6], the critical depth of cut or the location of the occurrence of grinding burn was investigated by the aid of nital etching, the evaluation of the increase of the BN amplitude, and the decrease of hardness on five workpieces with taper grinding.

It can be seen that the experimentally determined values for $e_{c,crit}$ were in the same range, but with the exception of one experimental point, which were all above the grinding burn limit determined by Malkin [25]. This makes the limits of the thermal surface and subsurface area influence appear plausible [26]. Nevertheless, workpieces in an industrial environment are often regarded as rejects before the occurrence of visible grinding burn which could be a sign of an unintentional beginning phase transformation. This results in the following procedure for micromagnetic analysis of thermally induced influences on surface integrity using the burning limit approach of Malkin are as follows. Although Malkin’s approach makes it possible to obtain indications of the occurrence of phase transformations, no statement can be made about the residual stress state, especially before visible grinding burn appeared. This is why it is necessary to detect a condition in which, primarily, only a displacement of residual stresses in the direction of tensile residual stresses or the occurrence of slight tensile residual stresses took place. Therefore, the often-cited stress sensitivity of the BN is used in the following to investigate Malkin’s model with regard to industrial relevant limits by aid of the root mean square value of the BN amplitude. Sridharan et al. [28] applied Malkin’s grinding energy partition model in conjunction with BN analysis to predict occurrence of thermal damage in through-hardened bearing steels independent of grinding variables. The new aspect of the following approach is the plot of the surface and subsurface property residual stress states versus the product $d_{eq}^{0.25} a_e^{-0.75} v_w^{-0.5}$ of Malkin’s. In this context, it was examined to what extent the measurand residual stress state was represented by the measured root mean square value of the BN in consideration of the micromagnetic analyzing depth.

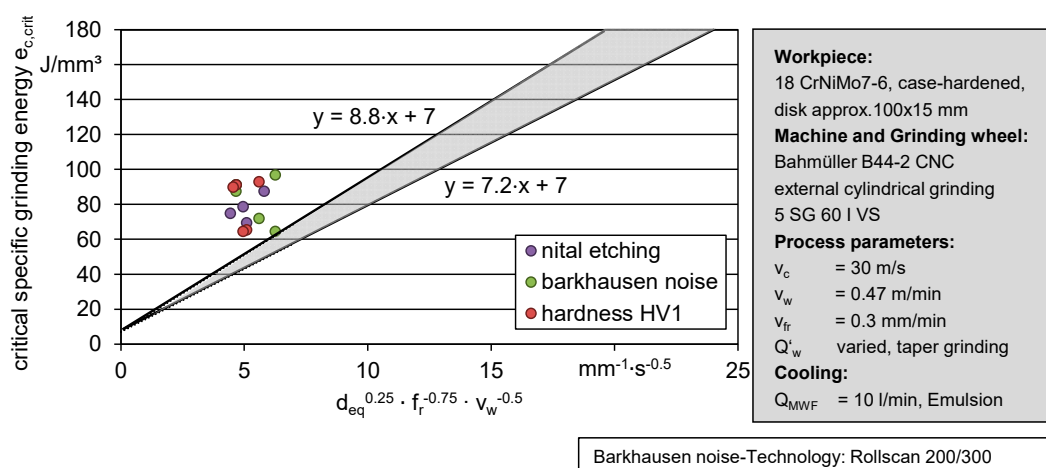


Figure 2. Comparison of the experimental results of thermally damaged workpieces identified by different methods with Malkin’s limits for thermal surface and subsurface area influence according to Reference [26].

In order to achieve this aim, specimens were ground under variation of process parameters and the corresponding specific grinding energy e_c was plotted versus the product $d_{eq}^{0.25} a_e^{-0.75} v_w^{-0.5}$ according to Malkin. Afterwards, the residual stress states of each experimental point were measured and represented above Malkin’s product $d_{eq}^{0.25} a_e^{-0.75} v_w^{-0.5}$. After, the dependency of the root mean square value of the BN on the residual stress state was checked.

3. Experimental Setup

In the context of this work, cylindrical case-hardened 18CrNiMo7-6 workpieces with seven separate sections, as shown in Figure 3, were machined by a cylindrical outer diameter grinding process with variation of relevant process parameters. The process-specific influenced material states of each section were measured by the micromagnetic BN method and compared with the results of residual stress measurements of a X-ray diffractometer (Seifert, type: 3000 PTS).

The grinding tests were carried out on a Studer S41 cylindrical grinding machine tool. The workpieces were clamped between centers. Oil as metal working fluid was used. The grinding experiments were carried out by use of a corundum grinding wheel A80CC5V (400 mm × 15 mm) in counter-direction with a constant fluid flow rate of Q_{MWF} of 40 L/min. The grinding wheel was dressed with a Chemical Vapour Deposition (CVD) form roller with a speed ratio q_d of 0.8 and a dressing overlap U_d of 4. During the grinding process, process forces (tangential force F_t , normal force F_n) were recorded by a piezoelectric measuring system integrated in the workpiece spindle and tailstock. In addition, the effective power of the grinding spindle was documented. The radial removal of the single-stage grinding process was 175 μm , which corresponded to a specific material removal volume V'_w of approximately 50 mm^3/mm . Due to the variation of the radial feed speed v_{fr} , the specific material removal rate Q'_w was set between 1 and 25 $\text{mm}^3/(\text{mm}\cdot\text{s})$ (Table 1).

Table 1. Experimental plan.

Material Condition	v_{fr} (mm/min)	Q'_w ($^3/(\text{mm}\cdot\text{s})$)
18 CrNiMo7-6 (AISI 4820) case-hardened, 58 HRC annealing temperature: 180 °C surface carbon content: 0.6% case hardening depth: 1.0 mm	0.2	1
	0.4	2
	0.8	4
	1.2	6
	1.6	8
	2.0	10
	2.4	12
	2.8	14
	3.2	16
	4.0	20
	4.4	22
	4.8	24
		5.0

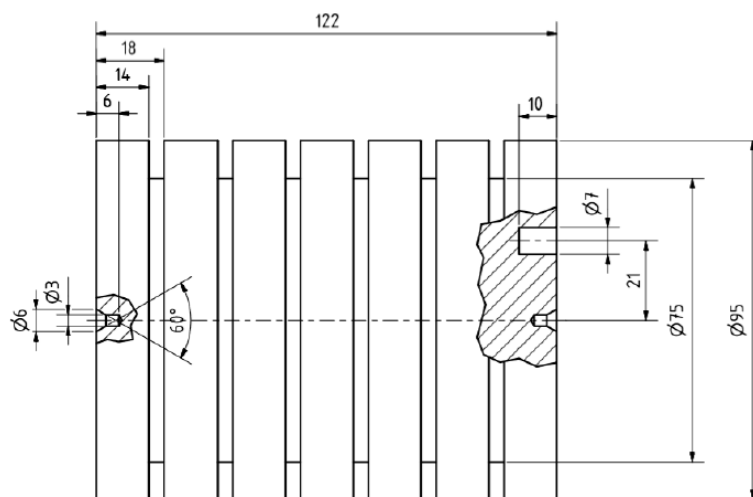


Figure 3. Geometry of the workpiece.

The cutting speed, v_c , and the workpiece speed, v_w , were kept constant with $v_c = 35$ m/s and a resulting speed ratio $q = 90$. These machining parameters were selected on the basis of empirical values from conventional external cylindrical grinding.

A Rollscan 350 from Stresstech was used for the micromagnetic workpiece analysis. In order to avoid handling influences on the BN measurements with the Rollscan technology, manual usage of the sensor should be avoided. Therefore, the Klingenberg P40 gear metrology center was used, which has

an inbuilt interface between the Rollscan 350 device and the specially designed BN sensor S1-14-12-29 (Figure 4).

By operating the travel axes, reproducible measurements can be made on slowly rotating workpieces clamped in a three-jaw chuck. The measurements were made with a magnetizing voltage of 5 V and a magnetizing frequency of 125 Hz. The analysis frequency range was 70–200 kHz. These magnetizing frequencies and analysis frequency ranges used in practice lead to an estimated analysis depth of approximately 20–50 μm , whereby a hardened martensitic microstructure of approximately 60 HRC is assumed. This estimation appears plausible according to the data of the analysis depths for soft and hard steels in Reference [10].

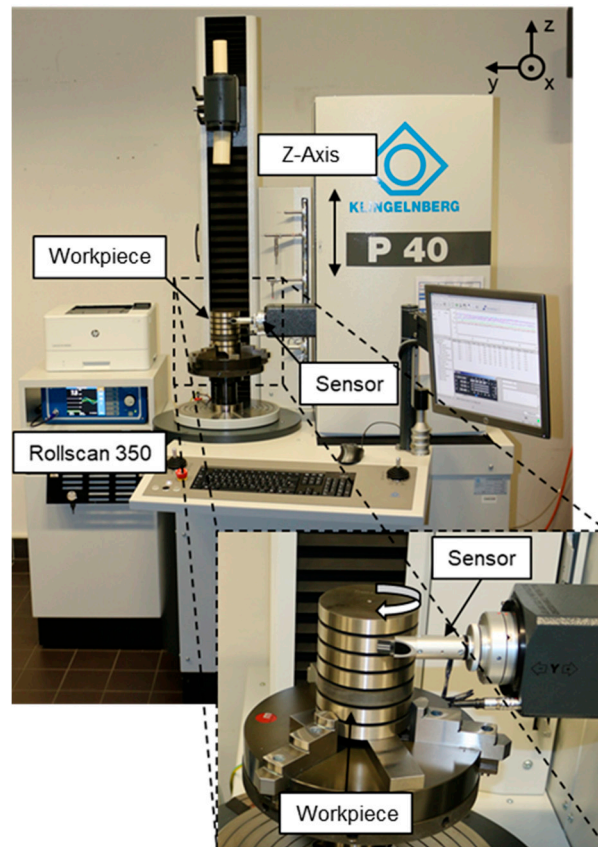


Figure 4. Barkhausen noise measurements on the Klingelberg P40 with Rollscan technology.

4. Results and Discussion

Figure 5 shows the specific grinding energy of the external cylindrical grinding tests plotted versus the product $d_{eq}^{0.25} a_e^{-0.75} v_w^{-0.5}$ according to Malkin. The product $d_{eq}^{0.25} a_e^{-0.75} v_w^{-0.5}$ was realized by the adjustment of different radial feed speeds, v_{fr} , and the resulting different nominal radial feeds, f_r , which corresponded, here, to the depth of cut a_e . Since, according to Equation (2), the grinding energy e_c depends on the measured tangential force F_t , it should be mentioned that the tangential force, F_t , can usually be measured with a standard deviation of less than 5% from three identically machined workpiece sections.

It can be seen that four experimental points (green) lie below or to the right of the grinding burn limits determined by Malkin [24,25]. One single experimental point (yellow) lies exactly between the two lines. All other experimental points (red) are located on or above the grinding burn limit line with a gradient of $8.8 \text{ J}/(\text{mm}^2 \cdot \text{s}^{0.5})$.

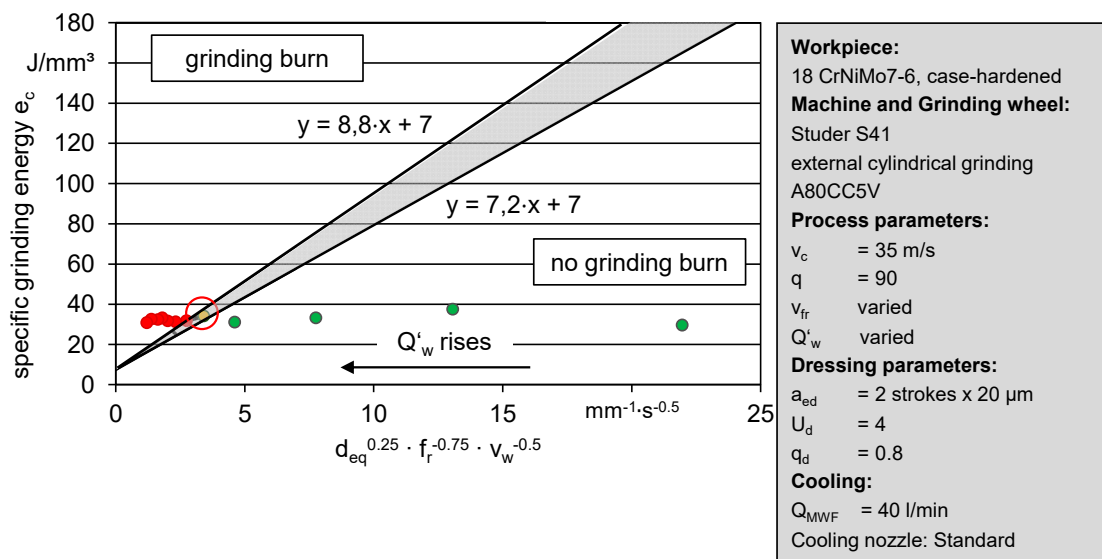


Figure 5. Comparison of experimental results with the limits for the thermal influence on the surface and subsurface area according to Malkin.

According to Malkin, the grinding experiments belonging to these experimental results must have produced rejected workpieces. Since it was the aim to detect an excess of the critical residual stress state of the surface and subsurface area with BN, the analysis depth of the BN was estimated at 50 μ m. Subsequently, residual stress depth curves in the grinding direction were prepared in four depth steps down to a depth of 50 μ m. Each measurement was measured with a standard deviation of less than 20 MPa. Afterwards, a residual stress state per surface and subsurface was determined by averaging over each depth profile. In order to calculate an averaged residual stress state, the integral of the depth profile from 0 μ m to 50 μ m was calculated and divided by 50 μ m.

Figure 6 shows the residual stress state (0–50 μ m) above the product $d_{eq}^{0.25} a_e^{-0.75} v_w^{-0.5}$. Of note is the experimental point from Figure 5 (see above), which lies between the two grinding limit lines of Malkin and was calculated with an average residual stress state of almost 0 MPa (Figures 5 and 6, red circle). While all experimental points lying on, above or left of the line of Malkin (red test points) have a tensile residual stress state, the residual stress state of all points lies below or right of the lines of Malkin (green experimental points) in the compression range. In addition, Figure 6 shows microsections of ground workpiece sections, which were machined with specific material removal rates Q'_w of 12 mm³/(mm·s) and 22 mm³/(mm·s). The microsections showed a visible annealing zone from approximately 10 μ m ($Q'_w = 12$ mm³/(mm·s)) to more than 50 μ m ($Q'_w = 22$ mm³/(mm·s)). The micrographs confirm the assignment of these experimental points to the grinding burn area.

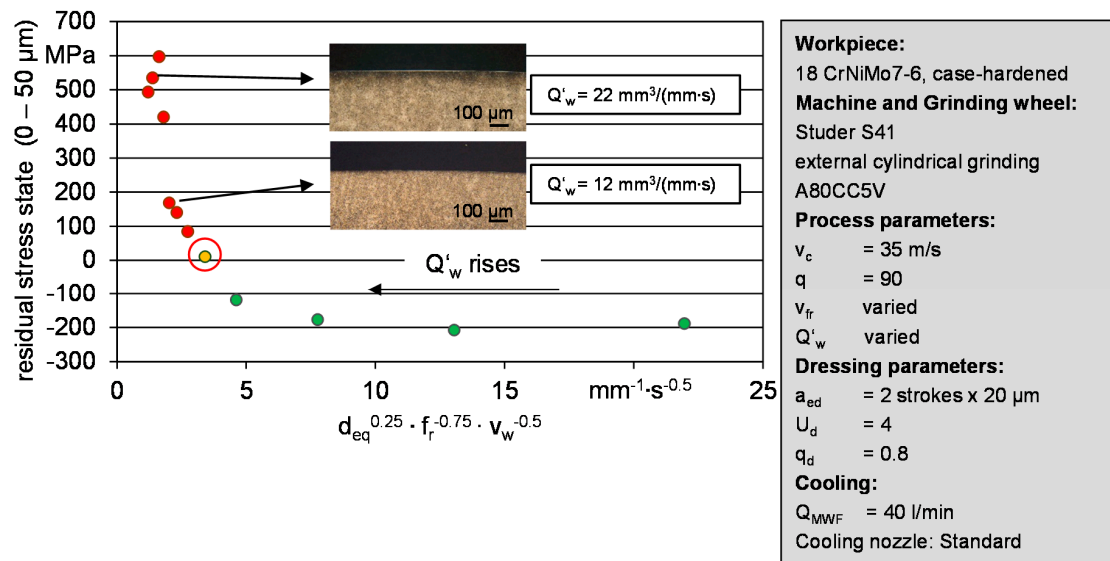


Figure 6. Residual stress state of the surface and subsurface area as a function of the product of $d_{eq}^{0.25} a_e^{-0.75} v_w^{-0.5}$.

In order to be able to determine the measurand residual stress state using the root mean square value of the BN amplitudes, named the *mp-value*, the correlation of the *mp-value* to the measured variable must be evaluated. Figure 7 shows the *mp-value* as a function of the residual stress state. The depicted *mp-values* were calculated as the averages of 1000 *mp-values* measured over the circumference of the workpiece. The error bars correspond to the standard deviation.

It can be seen that there was an approximately, proportional, and quadratic relationship among the residual stress displacement of the residual stress states from the compression range in the direction of the tension and even up to the tension range. This proportionality was disturbed at higher residual stresses. At higher thermomechanical loads, an increasing development of annealing zones and (Figure 6, microsections) a decrease in hardness was observed in Reference [29]. Thus, different material reactions must have a counteracting effect on the micromagnetic properties.

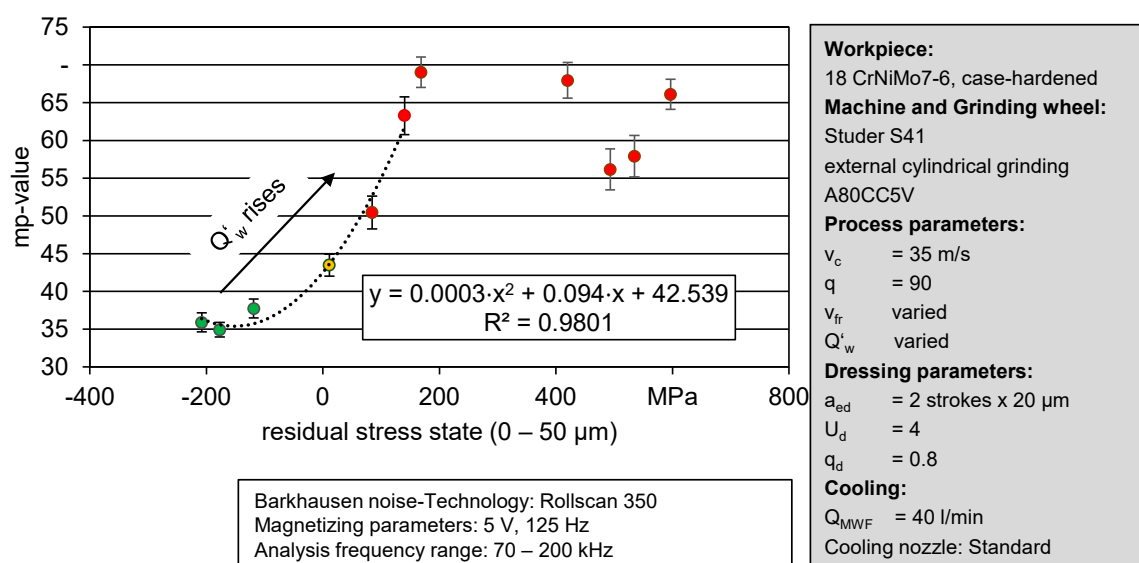


Figure 7. Residual stress sensitivity of the *mp-value*.

Due to the fact that tensile stresses possibly impair the functionality of ground parts by favoring the propagation of cracks, workpieces with tensile residual stresses in the surface and subsurface area are often regarded as rejected parts. An in-process monitoring and analysis of the power consumption using the process model developed by Malkin combined with a monitoring of the *mp-values* bear the capability for providing a reliable statement about the condition of the surface integrity of a ground workpiece. The procedure to deal with these criteria to differentiate between good and rejected parts is shown in Figure 8.

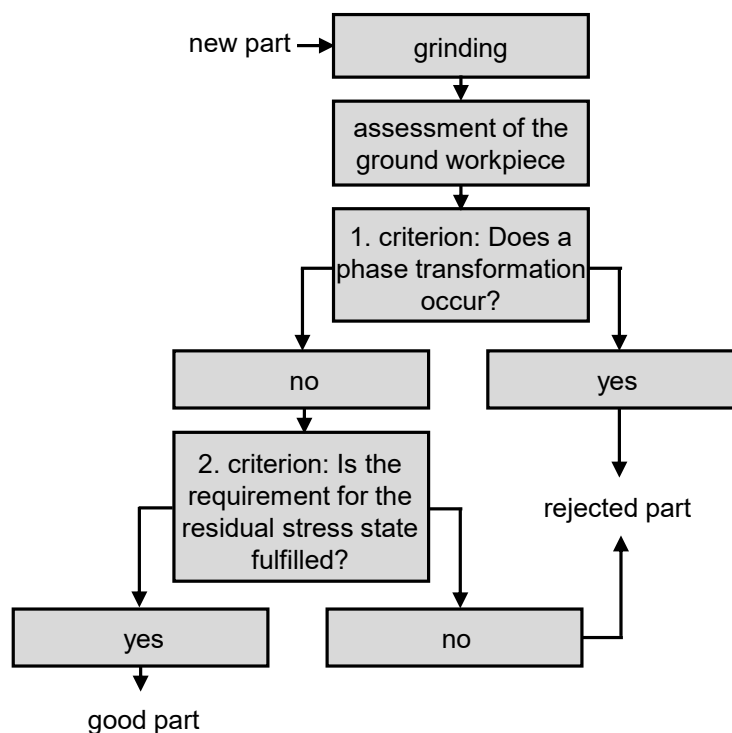


Figure 8. Application of the criteria to distinguish between good and rejected parts.

The question of the first criterion can be answered with “no” if the grinding burning limit of Malkin, which indicates the possibility of a beginning phase transformation, is not reached. The second criterion results in a good part when the requirement for the residual stress state in terms of the compliance of certain *mp-values* is fulfilled. This condition has to be previously defined by a calibration procedure. If the requirements for the residual stress state is 0 MPa, the threshold *mp-value* must be set to 44, as shown in Figure 7 (yellow experimental point). This assessment of ground workpieces is applicable in fast post-process mode and is suitable in an industrial multi-stage grinding process. After each process step, the current workpiece residual stress state can be checked, considering the process parameters and Malkin’s burning limit. This helps to achieve a process, which is as productive as possible, for example, the first stage of the grinding process was carried out in such a way that a part was indicated as rejected. Due to this fast post-process control, the following grinding steps can be adapted, so that the negative influenced surface and subsurface layers are removed in order to finally generate a good part.

Future research will focus on a setup for in-process measurements of BN. In the context of cylindrical outer diameter grinding experiments, the radial feed speed v_{fr} will be used for a controlled process based on in-process monitoring of BN considering the burning limit of Malkin.

5. Conclusions

Summary and Outlook

The combination of micromagnetic analysis with the use of the burning limit approach bears the capability of providing reliable information about the condition of the surface integrity of a ground workpiece. Our investigations showed that the residual stress state correlates with the product $d_{eq}^{0.25} a_e^{-0.75} v_w^{-0.5}$ of Malkin. The straight lines, according to Malkin, limit the residual stress state to 0 MPa after a single-stage cylindrical outer diameter grinding process. The results showed that, with measurements of the BN, incipient changes in the residual stress state up to industry-relevant limits are possible. The presented approach is suitable for application in a multi-stage grinding process in order to realize a fast post-process control process which is as productive as possible.

The obtained results must be verified in further experiments by varying the machining parameters or the product of $d_{eq}^{0.25} a_e^{-0.75} v_w^{-0.5}$, respectively, in the near future. In particular, the criteria of (1) Malkin’s grinding burn limit and (2) measurements of the BN have to be investigated. The transferability of the results to other material states, e.g., by varying control variables (annealing temperature) and result variables (case hardening depth, carbon content) of the case hardening process, must also be clarified.

In addition, the limits of Malkin’s model have to be investigated. The model is based on the assumption that a quasi-stationary temperature field is formed. According to previous knowledge, a certain workpiece length is necessary and a critical feed rate, v_w , of the workpiece must not be exceeded [24,30,31]. This must be checked, in particular, for the application of the model in more complex grinding processes with high workpiece feed rates (v_w).

In the future, the potential of a sensor system for in-process measurements of the BN will be evaluated. Furthermore, limits for the in-process measurement of the BN have to be determined, especially with regard to the response times of the sensor in connection with the feed rates (v_w) of the workpiece in the grinding process.

Author Contributions: The presented concept was developed by J.H. The specimen’s design, experimental setup, and measurements were performed by D.S. and J.H. The original draft was prepared by J.H., B.K. directed the study and contributed to the results interpretation, manuscript review and editing.

Funding: This research was funded by the DFG.

Acknowledgments: The scientific work has been supported by the DFG within the research priority program SPP 2086. The authors thank the DFG for this funding and intensive technical support. This work was done in project KA1006/28-1.

Conflicts of Interest: The authors declare no conflict of interest.

Nomenclature

Symbol	Unit	Designation
a	mm ² /s	thermal diffusivity
a_e	μm	depth of cut
a_{ed}	μm	depth of dressing
B	J/(mm ² s ^{0.5})	factor (Malkin)
$B(t)$	T	magnetic flux density
d_{eq}	Mm	equivalent wheel diameter
e_c	J/mm ³	specific grinding energy
$e_c^*, e_{c,crit}$	J/mm ³	critical specific grinding energy
e_w	J/mm ³	basis value of the specific grinding energy
F_n	N	normal force
F_t	N	tangential force
f_a	kHz	analyzing frequency

f_r	μm	nominal radial feed
$H(t)$	A/m	magnetic field strength
H_{cM}	A/m	coercivity
k	W/(m·K)	thermal conductivity
l	mm	half-length of source
$mp\text{-value}$	mV	magnetoelastic parameter
P_c	kW	grinding power
Q_{MWF}	l/min	metal working fluid flow rate
Q_w	mm^3/s	material removal rate
Q'_w	$\text{mm}^3/(\text{mm}\cdot\text{s})$	specific material removal rate
Q	W	heat flux
q	-	speed ratio (grinding)
q_d	-	speed ratio (dressing)
T	S	time
$U(t)$	V	voltage
U_d	-	dressing overlap
U_{ind}	mV	voltage
V	V	velocity of heat source
V'_w	mm^3/mm	specific material removal rate
v_c	m/s	cutting speed
v_{fr}	mm/min	radial feed speed
i	m/s	workpiece velocity
δ	μm	analyzing depth
μ_0	N/A ²	magnetic field constant
μ_r	H/m	relative permeability
σ	MPa	residual stresses/residual stress state
σ	1/($\Omega\cdot\text{m}$)	conductivity
θ_m	$^\circ\text{C}$, K	maximum temperature
θ_m^*	$^\circ\text{C}$, K	critical temperature

References

1. Thiemann, P.; Dollinger, C.; Goch, G. Untersuchungen zum Phänomen Schleifbrand. *HTM J. Heat Treat.* **2014**, *69*. [[CrossRef](#)]
2. Altpeter, I.; Boller, C.; Kopp, M.; Wolter, B.; Fernath, R.; Hirninger, B.; Werner, S. *Zerstörungsfreie Detektion von Schleifbrand mittels elektromagnetischer Prüftechniken*; Jahrestagung, Di.3.C.3.; DGZfP: Bremen, Germany, 2011.
3. Brinksmeier, E. Randzonenanalyse Geschliffener Werkstücke. Ph.D. Thesis, Universität Hannover, Hannover, Germany, 1982.
4. Karpuschewski, B. Mikromagnetische Randzonenanalyse Geschliffener Einsatzgehärteter Bauteile. Ph.D. Thesis, Universität Hannover, Hannover, Germany, 1995.
5. Karpuschewski, B.; Bleicher, O.; Beutner, M. Surface integrity inspection on gears using Barkhausen noise analysis. *Procedia Eng.* **2011**, *19*, 162–171. [[CrossRef](#)]
6. Meyer, L.W. Einsatz von Temperatur- und Kraftsensoren in Schleifwerkzeugen. Ph.D. Thesis, Universität Bremen, Bremen, Germany, 2006.
7. Schwienbacher, S. Einfluss von Schleifbrand auf die Flankentragfähigkeit einsatzgehärteter Zahnräder. Ph.D. Thesis, Technische Universität München, Munich, Germany, 2008.
8. Theiner, W.A. *Micromagnetic Techniques in Structural and Residual Stress Analysis by Nondestructive Methods*; Hauk, V., Ed.; Elsevier Science B.V.: Amsterdam, NY, USA, 1997.
9. Kneller, E. *Ferromagnetismus*; Springer: Berlin, Germany, 1962.
10. Suominen, L.; Woitijias, A. A comparative study of Barkhausen noise and X-ray diffraction measurements from ground ferritic steel samples. In Proceedings of the Fourth European Conference on Residual Stresses, Cluny en Bourgogne, France, 4–6 June 1996; pp. 243–250.

11. Theiner, W.A.; Schneider, E. *Bestimmung von (Eigen-) Spannungen mit magnetischen, magnetoelastischen und laufwegunabhängigen Ultraschallverfahren*; Fraunhofer-Gesellschaft zur Förderung der angewandten Forschung e.V.; Inst. für Zerstörungsfreie Prüfverfahren: Saarbrücken, Germany, 1979.
12. Neslusan, M.; Cizek, J.; Kolarik, K.; Minarik, P.; Cillikova, M.; Melikhova, O. Monitoring of grinding burn via Barkhausen noise emission in case-hardened steel in large bearing-production. *J. Mater. Process. Technol.* **2017**, *240*, 104–117. [[CrossRef](#)]
13. Jiles, D.C. Review of magnetic methods for nondestructive evaluation. *NDT Int.* **1988**, *21*, 311–319.
14. Gupta, H.; Zhang, M.; Parraka, A.P. Barkhausen effect in ground steels. *Acta Mater.* **1997**, *45*, 1917–1921. [[CrossRef](#)]
15. Regent, C.; Tönshoff, H.K. *Erkennung und Vermeidung von Schleifbrand beim Verzahnungsschleifen*; FVA 239 I, Heft 469; Forschungsvereinigung Antriebstechnik: Frankfurt, Germany, 1996.
16. Regent, C.; Tönshoff, H.K. *Industriefähiges Überwachungssystem zur Schleifbrandanalyse*; FVA 239 II, Heft 578; Forschungsvereinigung Antriebstechnik: Frankfurt, Germany, 1999.
17. Gorgels, C.; Schröder, T. *Untersuchung zur Schleifbarkeit unterschiedliche wärmebehandelter Einsatzstähle für die Zahnradfertigung*; FVA 329 III, Heft 841; Forschungsvereinigung Antriebstechnik: Frankfurt, Germany, 2008.
18. Santa-aho, S.; Vippola, M.; Sorsa, A.; Lindgren, M.; Latokartano, J.; Leiviskä, K.; Lepistö, T. Optimized laser processing of calibration blocks for grinding burn detection with Barkhausen noise. *J. Mater. Process. Technol.* **2012**, *212*, 2282–2293. [[CrossRef](#)]
19. Altpeter, I.; Tschuncky, R.; Szielasko, K. Electromagnetic techniques for materials characterization. In *Materials Characterization Using Nondestructive Evaluation (NDE) Methods*; Hübscher, G., Altpeter, I., Tschuncky, R., Herrmann, H.-G., Eds.; Woodhead Publishing: Cambridge, UK, 2016; pp. 225–262.
20. Thiemann, P. In- und Post-Prozess-Messverfahren für die Erfassung von thermo-mechanischen Schädigungen. Ph.D. Thesis, Universität Bremen, Bremen, Germany, 2019.
21. Sackmann, D.; Karpuschewski, B.; Epp, J.; Jedamski, R. Detection of surface damages in ground spur gears by non-destructive micromagnetic methods. *Forschung Ingenieurwesen* **2019**, *83*, 563–570. [[CrossRef](#)]
22. Karpuschewski, B. Sensors for Physical Properties. In *Sensors in Manufacturing*; Wiley-VCH: Weinheim, Germany; New York, NY, USA, 2001; pp. 123–142.
23. Tönshoff, H.K.; Karpuschewski, B.; Regent, C. Process monitoring in grinding using micromagnetic techniques. *Int. J. Adv. Manuf. Technol.* **1999**, *15*, 694–698. [[CrossRef](#)]
24. Malkin, S.; Guo, C. Thermal Analysis of Grinding. *CIRP Ann.* **2007**, *56*, 760–782. [[CrossRef](#)]
25. Malkin, S. Burning Limit for Surface and Cylindrical Grinding of Steels. *CIRP Ann.* **1978**, *27*, 233–236.
26. Brinksmeier, E.; Heinzl, C.; Meyer, L. Werkzeugseitige Temperatur- und Kraftsensoren zur Charakterisierung von Schleifprozessen. In *Jahrbuch Schleifen, Honen, Läppen und Polieren—Verfahren und Maschinen*; 63. Ausgabe; Hoffmeister, H.-W., Denkena, B., Eds.; Vulkan-Verlag GmbH: Essen, Germany, 2007; pp. 256–276.
27. Jaeger, J.C. Moving Sources of Heat and Temperature at Sliding Contacts. *Proc. R. Soc. New South Wales* **1942**, *76*, 263–274.
28. Sridharan, U.; Bedekar, V.; Kolarits, F.M. A functional approach to integrating grinding temperature modeling and Barkhausen noise analysis for prediction of surface integrity in bearing steels. *CIRP Ann.* **2017**, *66*, 333–336. [[CrossRef](#)]
29. Meyer, L.; Heinzl, C.; Brinksmeier, E. Monitoring of Grinding Processes Using a Sensor Equipped Grinding Wheel. *Ann. WGP* **2004**, *11*, 41–44.
30. Heinzl, C. *Schleifprozesse verstehen: Zum Stand. der Modellbildung und Simulation sowie unterstützender experimenteller Methoden*; Habilitationsschrift, Universität Bremen, Band 47; Shaker Verlag: Aachen, Germany, 2009.
31. Carslaw, H.; Jaeger, J.C. *Conduction of Heat in Solids*; Oxford Science Publications; Oxford University Press: Oxford, UK, 1959.

